

# Spectral Identification of the u-band Variable Sources in Two LAMOST fields

Tian-Wen Cao, Ming Yang, Hong Wu, Tian-Meng Zhang, Jian-Rong Shi, Hao-Tong Zhang, Fan Yang, Jing-Kun Zhao, Xu Zhou, Zhou Fan, Zhao-Ji Jiang, Jun Ma, Jia-Li Wang, Zhen-Yu Wu, Hu Zou, Zhi-Min Zhou, Jun-Dan Nie, A-Li Luo, Xue-Bing Wu, Yong-Heng Zhao

## ABSTRACT

We selected 82 u-band variable objects based on the u-band photometry data from SCUSS and SDSS, in the field of LAMOST Complete Spectroscopic Survey of Pointing Area at Southern Galactic Cap. The magnitude variation of the targets is restricted to larger than 0.2 mag and limiting magnitude down to 19.0 mag in u-band. According to the spectra from LAMOST, there are 11 quasars with redshift between 0.4 and 1.8, 60 variable stars and 11 unidentified targets. The variable stars include one active M-dwarf with a series of Balmer emission lines, seven Horizontal Branch stars containing six RR Lyrae stars matching with SIMBAD, and one giant, one AGB star and two RR Lyrae candidates by different color selections. All these variable stars mainly locate near the main sequence in the  $g - r$  vs.  $u - g$  diagram. The quasars are well distinguished from stars by both  $u - g$  color and variation in u-band.

*Subject headings:* quasars: general — stars: general — stars: statistics

## 1. Introduction

Recent large surveys have provided astronomers an unprecedented opportunity in the field of the time-domain astronomy. The two current large projects of Pan-STARRS(Kaiser et al. 2002) and The Palomar Transient Factory( PTF; Law et al.

---

<sup>1</sup>Key Laboratory of Optical Astronomy, National Astronomical Observatories, Chinese Academy of Sciences, Beijing 100012, P.R. China

2009), which cover large field of sky, have an ability to search many classes of variable objects with different timescales. The future Large Synoptic Survey Telescope (LSST; Ivezić et al. 2008; LSST Science Collaboration et al. 2009) can further increase the number of variable objects in several order of magnitudes. Though the photometry of multiple observations with different timescales can identify many variable objects, especially periodic variable stars, such as RR Lyrae, eclipsing binaries, and Delta Scuti, etc, spectral identification is still an important tool to verify some other types of variable objects, for example, quasars.

Some works have been done before on the Stripe 82 (Ivezić et al. 2007; Bramich et al. 2008; Bhatti et al. 2010), which is an important region of the Sloan Digital Sky Survey (SDSS York et al. 2000) covered about  $290\text{-degree}^2$  on the celestial equator in the Southern Galactic Hemisphere. This region has been observed 10 times on average and many variable sources such as quasars, RR Lyrae stars, giant stars, eclipsing binaries have been confirmed by both photometry and spectroscopy.

Generally, quasars and blue stars are observed more effectively in u-band than in other optical bands, since their luminosities or variations in u-band are physically larger than those in other optical bands (Davenport et al. 2012). Based on these features, quasars and some variable stars (such as RR Lyrae stars) are easily distinguished from others in the color-color diagram of  $g - r$  vs.  $u - g$  (Richards et al. 2002; MacLeod et al. 2011).

The South Galactic Cap u-band Sky Survey (SCUSS) (Zou et al. 2015a) is a project which finally performs sky survey of about  $5000\text{-degree}^2$  of the South Galactic Cap in u-band by using 2.3m Bok Telescope and the area is also almost covered by SDSS. Taking advantage of the u-band variation between SDSS and SCUSS, many variable objects (ex. quasars Zou et al. 2015b) can be selected. However the large follow-up spectral identifications should only depend on the large spectral survey programs.

The Large Sky Area Multi-Object Fiber Spectroscopic Telescope (LAMOST, also known as Guoshoujing telescope, GSJT, Wang et al. 1996; Su & Cui 2004; Cui et al. 2012; Zhao et al. 2012) is a Wang-Su Schmidt telescope located in Xinglong Station of National Astronomical Observatory, Chinese Academy of Sciences (NAOC). LAMOST is a special reflecting Schmidt telescope with the correcting mirror Ma and the primary mirror Mb. An innovative active optics technique is utilized

by LAMOST and it can achieve a series different reflecting Schmidt systems by changing its mirror surface continuously. With 4-meter clear aperture, 20-degree<sup>2</sup> field of view (FOV) and 4000 fibers, it is able to simultaneously spectroscopically observe more than 3000 scientific targets in a single exposure. This highly efficient facility will survey a large volume of space (including SCUSS area) for both stars and galaxies. By taking advantage of large area and multi-object fiber of LAMOST, the spectra of u-band variables can be acquired efficiently.

The LAMOST Complete Spectroscopic Survey of Pointing Area (LCSSPA) at Southern Galactic Cap (SGC) is a LAMOST Key Project which designed to spectroscopically observe all sources (Galactic and extra-galactic) with limiting magnitude of  $r = 18.1 \text{ mag}$  by selecting two 20-degree<sup>2</sup> FOVs at the SGC. The survey mainly aims at completeness of the LAMOST Extra GALactic Survey (LEGAS). Meanwhile, besides of the normal galaxy survey, many scientific research fields are also included, such as the studies of galaxy clusters, luminous infrared galaxies, and time-series variable sources (u-band variables and quasars). Thus the spectral identification of u-band variable sources of LCSSPA can be treated as a precursor research in future large program.

In this paper, we identify the u-band variables by their spectra in two fields of LCSSPA. The sample selection, observation and data reduction are presented in §2. The spectral identification are described in §3. In §4, we analyze the color and spectral characteristics of u-band variables, and discuss the reliability and efficiency of quasar selection. The summary is given in §5.

## 2. Sample Selection, Observation and Data Reduction

The LCSSPA covers two 20-degrees<sup>2</sup> areas with central coordinates at  $R.A. = 37.88^\circ$ ,  $Dec. = 3.44^\circ$  (Field A) and  $R.A. = 21.53^\circ$ ,  $Dec. = -2.20^\circ$  (Field B). These two areas are in the overlapping field of SCUSS and SDSS. Thus, we are able to take spectroscopic observation of selected u-band variables in two LCSSPA fields. The targets in the FOV are mainly constituted of stars, galaxies, quasars, u-band variables and HII regions. According to their r-band magnitude, all targets in the FOV are divided into two kinds of plate, bright (B) plate, ( $14.0 \sim 16.0 \text{ mag}$ ) and faint (F) plate, ( $16.0 \sim 18.1 \text{ mag}$ ). The observations have been conducted from

Sep 2012 to Jan 2014. The Field A was observed with 5 B and 12 F plates, and Field B was observed with 6 B and 5 F plates. The raw data have been reduced with LAMOST 2D and 1D pipelines (Luo et al. 2012, 2014) which including bias subtraction, flat-fielding through twilight exposures, cosmic-ray removal, spectrum extraction, wavelength calibration, sky subtraction and exposure coaddition.

The u-band limiting magnitude of the SCUSS is  $\sim 23.2$  mag which is about 1.5 mag deeper than that of SDSS. Based on the performance of LAMOST, we have restricted u-band photometry PSF magnitude down to 19.0 mag. Then, the coordinates of all targets in the FOV are matched between the SDSS and SCUSS data within one arcsecond. The final error ( $\sigma$ ) of the magnitude variation in u-band combines both errors of SCUSS and SDSS, and the fitting of the  $3\text{-}\sigma$  errors of all targets is shown as red dashed lines in Figure.1. Here, a criterion of 0.2 magnitude is adopted to select the u-band variable objects.

All the objects have been inspected via SDSS images and flags to eliminate those with bad photometry. The targets with any nearby objects less than 2-arcsec are eliminated too. Finally, There are 82 u-band variable sources are observed by LAMOST (see Figure1).

### 3. Identification of u-band Variable Objects

#### 3.1. Quasar

Quasars are identified by their broad band emission lines: such as [CIV]  $\lambda 1549$ , [CIII]  $\lambda 1909$ , MgII  $\lambda 2800$ , H $\gamma$   $\lambda 4340$ , H $\beta$   $\lambda 4861$ , H $\alpha$   $\lambda 6563$ . There is a total of 11 quasars out of 82 variable sources. The redshifts are measured manually on LAMOST spectra with at least two emission lines, including above broad emission lines and some narrow emission lines such as [OIII]  $\lambda\lambda 4959, 5007$ . The errors of redshifts are less than 0.001. The redshifts of quasars are between 0.4 and 1.8. All the information of quasars are listed in Table 2. Four quasars have been found in NED, among which two have also been observed by SDSS. The rest of seven quasars are newly discovered. The Figure2 shows the spectra of 11 quasars.

### 3.2. Variable stars

60 u-band variable stars have been identified by their optical spectra. The rest of 11 sources are unidentified due to the low signal-to-noise rate (SNR) of spectra. Figures 3-4 show all the spectra of these stars.

The MILES library (Sánchez-Blázquez et al. 2006; Vazdekis et al. 2010) which contains 985 high SNR low-resolution observed stellar spectra, provides important parameters of different stellar subtypes. MILES can be used as a source of templates to classify stellar spectra (Zhao et al. 2011). We have used the MILES library as the spectral template to cross-match with the spectra of 60 variable stars and determine their spectral types. The template matching is mainly based on the typical spectral profile and absorption lines. There are 5 A-type, 12 F-type, 32 G-type, 6 K-type and 5 M-type stars have been identified according to the template matching.

Meanwhile, the 60 variable stars are also cross-matched with LAMOST Date Release Two (DR2) which including the stellar parameters of effective temperature, surface gravity and  $[\text{Fe}/\text{H}]$  derived by the LASP pipeline (Wu et al. 2014). There are 51 objects matched and the distribution of spectral types is similar to the one derived from the use of MILES templates. Also, we have identified five M-dwarf including one active M-dwarf **J022727.49+031054.8** with strong Balmer emission series ( $\text{H}8$ ,  $\text{H}\epsilon$ ,  $\text{H}\delta$ ,  $\text{H}\gamma$ ,  $\text{H}\beta$ ,  $\text{H}\alpha$ ) and  $[\text{CaII}]$  HK lines by spectral inspection.

After spectral classification, we cross-matched all these variable sources with SIMBAD (Wenger et al. 2000) except for quasars. There are seven Horizontal Branch stars including six RR Lyrae stars and one variable star candidate. And on the basis of color selection of RR Lyrae (Ivezić et al. 2005) and other variable stars (Yanny et al. 2009; Bhatti et al. 2010), we also selected one AGB, one giant and other two RR Lyrae star candidates. Table 1 shows the criteria of color-color selection of stars. Table 2 lists the general properties of all u-band variables including their spectral types.

## 4. Discussion

### 4.1. Optical Color Diagrams

Due to warning flags in some bands of SDSS photometric data, only 39 stars, 11 quasars and 9 unidentified sources can be shown in the  $g - r$  vs.  $u - g$  diagram in Figure 5. From the diagram, the positions of variable sources show that variable stars are located near the main sequence and quasars appear at the region consistent with previous works on Stripe 82 (Sesar et al. 2007). The variable sources which show up near the main sequence may be some eclipsing binary or some activity outbreaks (e.g. a magnetic storm in an M-type dwarf). For the unidentified sources, there is a need for follow-up observations in future studies.

In the Figure, we can see that the characteristic color of quasars is  $u - g \leq 0.6$  which is consistent with low-redshift quasars in SDSS (Ivezić et al. 2003). Combining with  $u - g$  color criteria and u-band magnitude variation  $\geq 0.2$  mag, quasars can be almost completely identified. Of course, some variables will be missed by setting the u-band magnitude variation  $\geq 0.2$  mag.

### 4.2. Reliability of Variation

Since the u-band filter of SCUSS is slightly bluer than SDSS and the flux calibration of SCUSS-u did not consider the color term, there exists a systematic magnitude difference between SCUSS and SDSS in u-band and the difference depends on  $u - g$  color of targets. Based on the Equation 3 of Zou et al. (2015a), the systematic differences of all the variable stars in this paper are less than 0.026 mag with  $u - g$  values from 0.8 to 2.5. If we adopt the Equation 1 of Zou et al. (2015b), the systematic differences are less than 0.036 mag. Therefore the systematic error of variable stars is less than 0.04 mag.

Meanwhile the magnitude difference of quasars changes with the redshift. Zou et al. (2015b) showed the changes with redshift in their Figure 5. The maximum of magnitude difference of composite quasar spectra is about 0.06 mag at redshift of 1.5 for low-redshift quasars ( $z < 2$ ) and less than 0.03 mag at redshift of  $z < 1.5$ . Even considering some special quasars, the magnitude difference is less than 0.12 mag. As our

quasars are all low-redshift ( $z < 2$ ), only two of them have redshifts larger than 1.5. However the two u-band magnitude variations are 0.232 and 0.252 mag respectively, their variations are still much higher than the possible systematic differences.

Because the SCUSS is about 1.5 magnitudes deeper than SDSS in u-band, the photometric error of SCUSS are far below that of SDSS. The final error of magnitude variation is dominated by SDSS. Generally, most sample variable sources have errors less than 0.05 mag, and only a few of them could reach 0.08 mag. Considering both systematic error and measurement error, it is quite safe to set a criteria of 0.2 mag to select variable sources in u-band. The variations are more than three times of measurement errors, and also much higher than systematic errors even considering the worst case.

### 4.3. The Spectra of Variable Stars

Most absorption lines of stars appear at the spectral wavelengths in the LAMOST blue arm, so the SNR of blue arm is more important. However only 22 stars have SNRs of higher than 20 in blue arm, we mainly focus on the analysis of the absorption lines in these stars.

There are four RR Lyr stars and one of them have three spectra obtained by different nights. The RR Lyr star (Chadid & Gillet 1996) is a kind of pulsational variable star whose luminosity, color and radial velocity periodically vary during the pulsation. The figure 6 shows the  $H\gamma$ ,  $H\beta$  and  $H\alpha$  profile of **J013016.71-024240.2** in different day (possibly different phases). In  $H\alpha$  spectra, it also presents the obviously fill-in  $H\alpha$  emission line (Yang et al. 2014) in two nights. The  $H\alpha$  emission relates with the heating of shock wave at different phase (Gillet & Fokin 2014).

Additional 10 variable stars' spectra are late F-type or early G-type, shown in Figure 7. Their spectra show [Ca II] HK lines and G-band, which is caused by molecule CH (from  $\lambda 4295$  to  $\lambda 4315$ ), and weak balmer series features and the metallic lines. Those features are similar to the typical spectrum of G0V (Morgan et al. 1978).

The other 8 variable stars' spectra are late G-type and K-type star. The G-type stars show some lines sensitive with luminosity such as the G-band of CH and Sr II ( $\lambda 4077$ ) (Keenan & McNeil 1976). However few of our spectra stars show strong

SrII feature of G-type. Furthermore the MgH( $\lambda$ 4780) can clearly be seen late-K-type(Jaschek & Jaschek 1987) stars. Figure 8 shows examples of a G-type star with SrII feature and a late K-type star.

Based on the stellar parameters acquired from the LAMOST DR2, most of variables are main sequence stars and this is consistent with the result in the color-color diagram.

#### 4.4. The Method and Efficiency of Quasar Selection

Sesar et al. (2007) employed the multi-color method to select the variable sources in Stripe 82. More than 95% of them are low-redshift quasars, RR Lyrae stars and main sequence stars. Due to the field of stripe 82 has multi-time observations, Bhatti(Bhatti et al. 2010) has utilised the light-curve to study the variable sources and these variable sources include quasars and periodic variables(e.g. eclipsing binary systems, RR Lyrae and Delta Scuti candidates). Schmidt et al. (2010) parameterized the single-band variability by a model of the light-curve to select quasars at  $2.5 < z < 3.0$  with high efficiency. Peters et al. (2015) combines color and variability information to select quasars and the method effectively improves the selection of the quasars at  $2.7 < z < 3.5$ . Though Pan-STARRS1(PS1) survey provides multi-color(grizy) observation, it is not quite efficiency to select quasars in lower redshift without u-band. However the variability from multi-epoch observations will greatly increase the efficiency(Morganson et al. 2014).

In all, combining with both multi-color and variability will provide a high efficiency method to select quasars. However we only have two-epoch with gap of four to twelve years (Table 2) and we can only obtain the variation instead of variability of sources. Fortunately, most quasar present the variation in timescale of years(Sesar et al. 2007) and u-band is very sensitive to the variation of quasar at lower redshift. With criteria of  $u - g \leq 0.6$  and magnitudes difference  $\geq 0.2$  mag in u-band, we identified 11 quasars from 12 candidates by LAMOST spectra, with an efficiency of 91.7%. At high galactic latitude of LCSSPA, sources with  $u - g \leq 0.6$  are mainly quasars and white dwarfs. Because the variation of white dwarfs are too small to reach 0.2 mag, we believe the left one is still a real quasar. To explain the critical role of variation in u-band, we compare the efficiency by only  $u - g$  selection



at the same field. With  $u - g \leq 0.6$ , we have 155 sources with LAMOST spectra. Except the 59 unidentified sources, we identified 48 quasars. The efficiency to select quasars is only about 30%. Though the sample may be not enough to give the true efficiency of the method, it is a quite efficient way. However, we missed most quasars in this field. The possible reason is that many quasars could have variation far less than 0.2 mag at the two-epoch in u-band. The quasar selection with two-epoch variation more than three times the photometric errors (Zou et al. 2015b) in overlapping field of SCUSS and SDSS at the South Galactic Cap would overcome part of our incompleteness.

In recent future, many multi-epoch survey programs would focus on variable sources. However, all these surveys (such as PS1, LSST, etc on) do not include u-band. Therefore, the u-band of both SCUSS and SDSS is an unique and important band to help us to separate the quasars ( $z < 2$ ) and variable stars by criteria of either color or variation.

## 5. Summary

In this paper, we selected a sample of 82 u-band variables in the region of LCSSPA based on criteria of u-band magnitude variation  $\geq 0.2$  mag and the SCUSS u-band magnitude brighter than 19.0 mag. After spectral identification, there are 11 quasars with redshift between 0.4 and 1.8, 60 variable stars and 11 unidentified sources. Among the variable stars, there is one active M-dwarf, which present a series of strong Balmer emission lines; There are seven HB star including six RR Lyrae stars and one variable star candidate matching with SIMBAD; one AGB, one giant and two RR Lyrae candidates by multi-color diagnostic tools. Basing on the analysis of the reliability and efficiency, we conclude that the criteria of both  $u - g \leq 0.6$  and u-band variation above 0.2 mag is quite an efficiency to select quasar at redshift less than 2.

## Acknowledgments

This project is supported by the China Ministry of Science and Technology under the State Key Development Program for Basic Research (2014CB845705, 2012CB821800); the National Natural Science Foundation of China (Grant No.11173030, 11225316); the Strategic Priority Research Program "The Emergence of Cosmological Structures" of the Chinese Academy of Sciences (Grant No.XDB09000000); the Guoshoujing Telescope Spectroscopic Survey Key Projects; Wu,Z.Y. was supported by the Chinese National Natural Science Foundation (Grant Nos. 11373033).

Guoshoujing Telescope (the Large Sky Area Multi-Object Fiber Spectroscopic Telescope, LAMOST) is a National Major Scientific Project built by the Chinese Academy of Sciences. Funding for the project has been provided by the National Development and Reform Commission. LAMOST is operated and managed by the National Astronomical Observatories, Chinese Academy of Sciences.

The SCUSS is funded by the Main Direction Program of Knowledge Innovation of Chinese Academy of Sciences (No. KJCX2-EW-T06). It is also an international cooperative project between National Astronomical Observatories, Chinese Academy of Sciences and Steward Observatory, University of Arizona, USA. Technical supports and observational assistances of the Bok telescope are provided by Steward Observatory. The project is managed by the National Astronomical Observatory of China and Shanghai Astronomical Observatory.

## REFERENCES

- Bhatti, W. A., Richmond, M. W., Ford, H. C., & Petro, L. D. 2010, *ApJS*, 186, 233
- Bramich, D. M., Vidrih, S., & Wyrzykowski, L. 2008, *MNRAS*, 386, 887
- Chadid, M. & Gillet, D. 1996, *A&A*, 315, 475
- Cui, X.-Q., Zhao, Y.-H., & Chu, Y.-Q. 2012, *Research in Astronomy and Astrophysics*, 12, 1197
- Davenport, J. R. A., Becker, A. C., & Kowalski, A. F. 2012, *ApJ*, 748, 58
- Gillet, D. & Fokin, A. B. 2014, *A&A*, 565, A73
- Ivezić, Ž., Lupton, R. H., & Anderson, S. 2003, *Mem. Soc. Astron. Italiana*, 74, 978
- Ivezić, Ž., Smith, J. A., & Miknaitis, G. 2007, *AJ*, 134, 973
- Ivezic, Z., Tyson, J. A., & Abel, B. 2008, *ArXiv e-prints*
- Ivezić, Ž., Vivas, A. K., Lupton, R. H., & Zinn, R. 2005, *AJ*, 129, 1096
- Jaschek, C. & Jaschek, M. 1987, *The classification of stars*
- Kaiser, N., Aussel, H., & Burke, B. E. 2002, in *Society of Photo-Optical Instrumentation Engineers (SPIE) Conference Series*, Vol. 4836, *Survey and Other Telescope Technologies and Discoveries*, ed. J. A. Tyson & S. Wolff, 154–164
- Keenan, P. C. & McNeil, R. C. 1976, *An atlas of spectra of the cooler stars: Types G,K,M,S, and C. Part 1: Introduction and tables*
- Law, N. M., Kulkarni, S. R., & Dekany, R. G. 2009, *PASP*, 121, 1395
- LSST Science Collaboration, Abell, P. A., & Allison, J. 2009, *ArXiv e-prints*
- Luo, A., Zhang, J., & Chen, J. 2014, in *IAU Symposium*, Vol. 298, *IAU Symposium*, ed. S. Feltzing, G. Zhao, N. A. Walton, & P. Whitelock, 428–428
- Luo, A.-L., Zhang, H.-T., & Zhao, Y.-H. 2012, *Research in Astronomy and Astrophysics*, 12, 1243

- MacLeod, C. L., Brooks, K., & Ivezić, Ž. 2011, *ApJ*, 728, 26
- Morgan, W. W., Abt, H. A., & Tapscott, J. W. 1978, Revised MK Spectral Atlas for stars earlier than the sun
- Morganson, E., Burgett, W. S., Chambers, K. C., & Green, P. J. 2014, *ApJ*, 784, 92
- Peters, C. M., Richards, G. T., Myers, A. D., & Strauss, M. A. 2015, *ApJ*, 811, 95
- Richards, G. T., Fan, X., & Newberg, H. J. 2002, *AJ*, 123, 2945
- Sánchez-Blázquez, P., Peletier, R. F., & Jiménez-Vicente, J. 2006, *MNRAS*, 371, 703
- Schmidt, K. B., Marshall, P. J., Rix, H.-W., Jester, S., Hennawi, J. F., & Dobler, G. 2010, *The Astrophysical Journal*, 714, 1194
- Sesar, B., Ivezić, Ž., & Lupton, R. H. 2007, *AJ*, 134, 2236
- Su, D.-Q. & Cui, X.-Q. 2004, *Chinese J. Astron. Astrophys.*, 4, 1
- Vazdekis, A., Sánchez-Blázquez, P., & Falcón-Barroso, J. 2010, *MNRAS*, 404, 1639
- Wang, S.-G., Su, D.-Q., Chu, Y.-Q., Cui, X., & Wang, Y.-N. 1996, *Appl. Opt.*, 35, 5155
- Wenger, M., Ochsenbein, F., & Egret, D. 2000, *A&AS*, 143, 9
- Wu, Y., Luo, A., & Du, B. 2014, *ArXiv e-prints*
- Yang, F., Deng, L., & Liu, C. 2014, *New A*, 26, 72
- Yanny, B., Rockosi, C., & Newberg, H. J. 2009, *AJ*, 137, 4377
- York, D. G., Adelman, J., & Anderson, Jr., J. E. 2000, *AJ*, 120, 1579
- Zhao, G., Zhao, Y.-H., & Chu, Y.-Q. 2012, *Research in Astronomy and Astrophysics*, 12, 723
- Zhao, J.-K., Zhao, G., Chen, Y.-Q., & Luo, A.-L. 2011, *Research in Astronomy and Astrophysics*, 11, 563
- Zou, H., Jiang, Z., & Zhou, X. 2015a, *AJ*, 150, 104

Zou, H., Wu, X.-b., & Zhou, X. 2015b, PASP, 127, 94

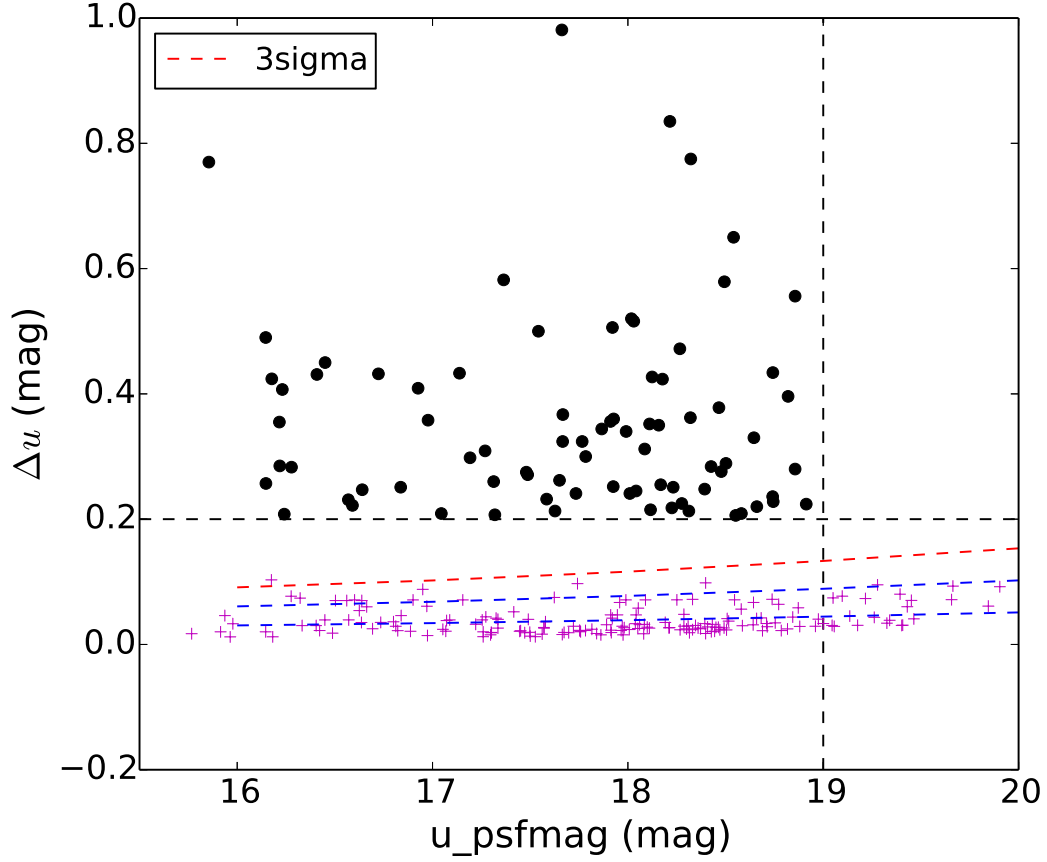


Fig. 1.—: Diagram of magnitudes versus variation in u-band. The plus signs (+) represent the standard deviation ( $\sigma$ ) of magnitude variation. The red dashed line represents the fitting of 3- $\sigma$  errors by second order polynomial. The black dots represent 82 u-band variable objects. The dashed lines are selection criteria:  $u < 19$  and  $\Delta u > 0.2$ .

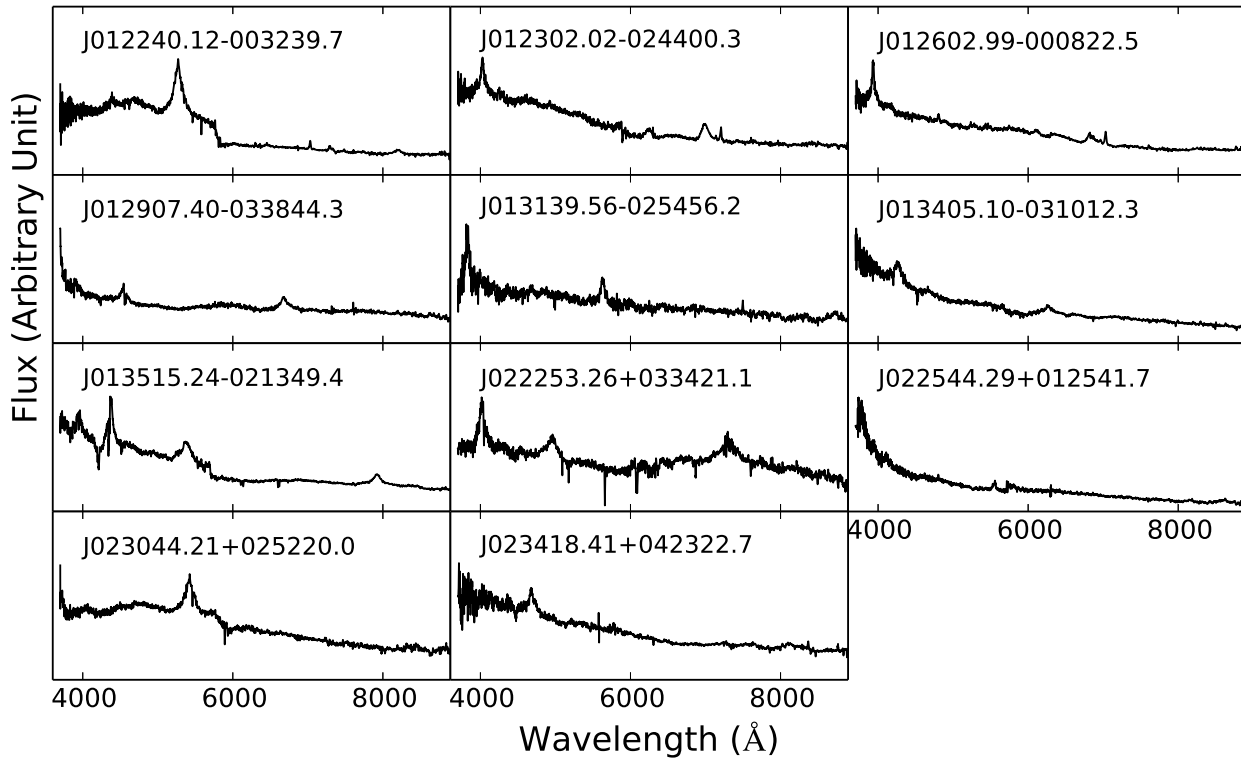


Fig. 2.—: The spectra of 11 variable quasars from LCSSPA.

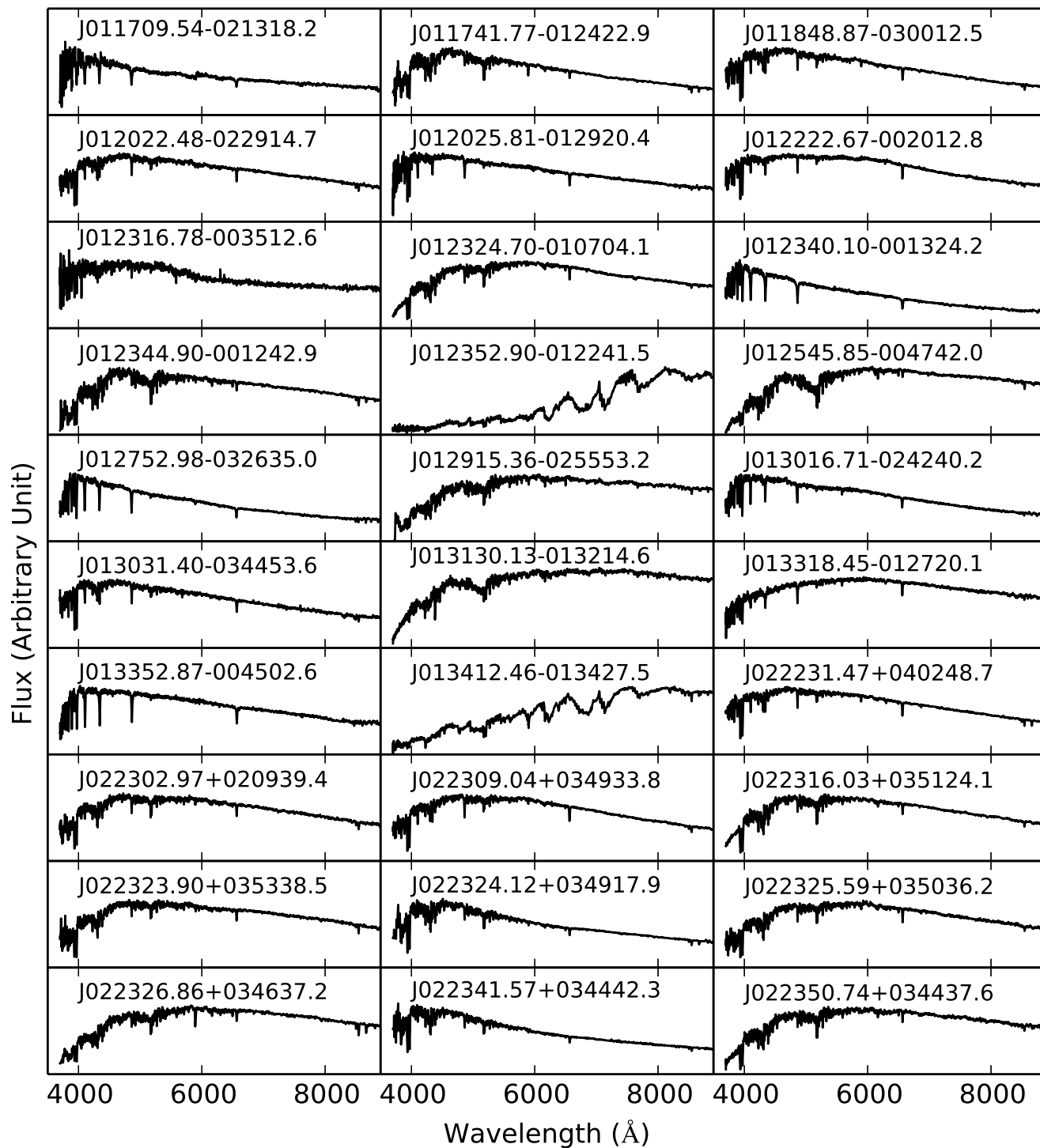


Fig. 3.— The spectra of variable stars in u-band from LCSSPA.



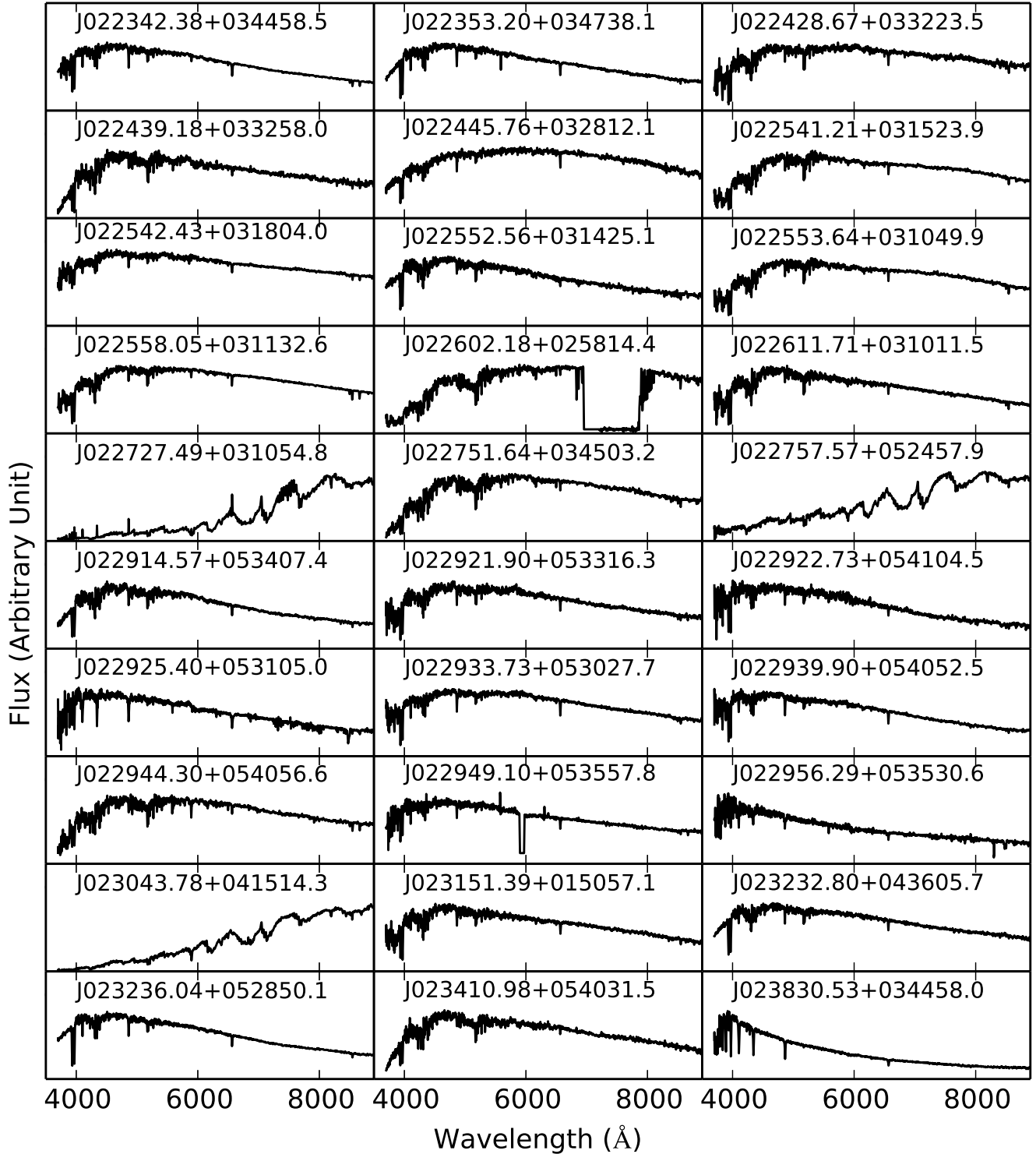


Fig. 4.—: The Same as Figure 3.

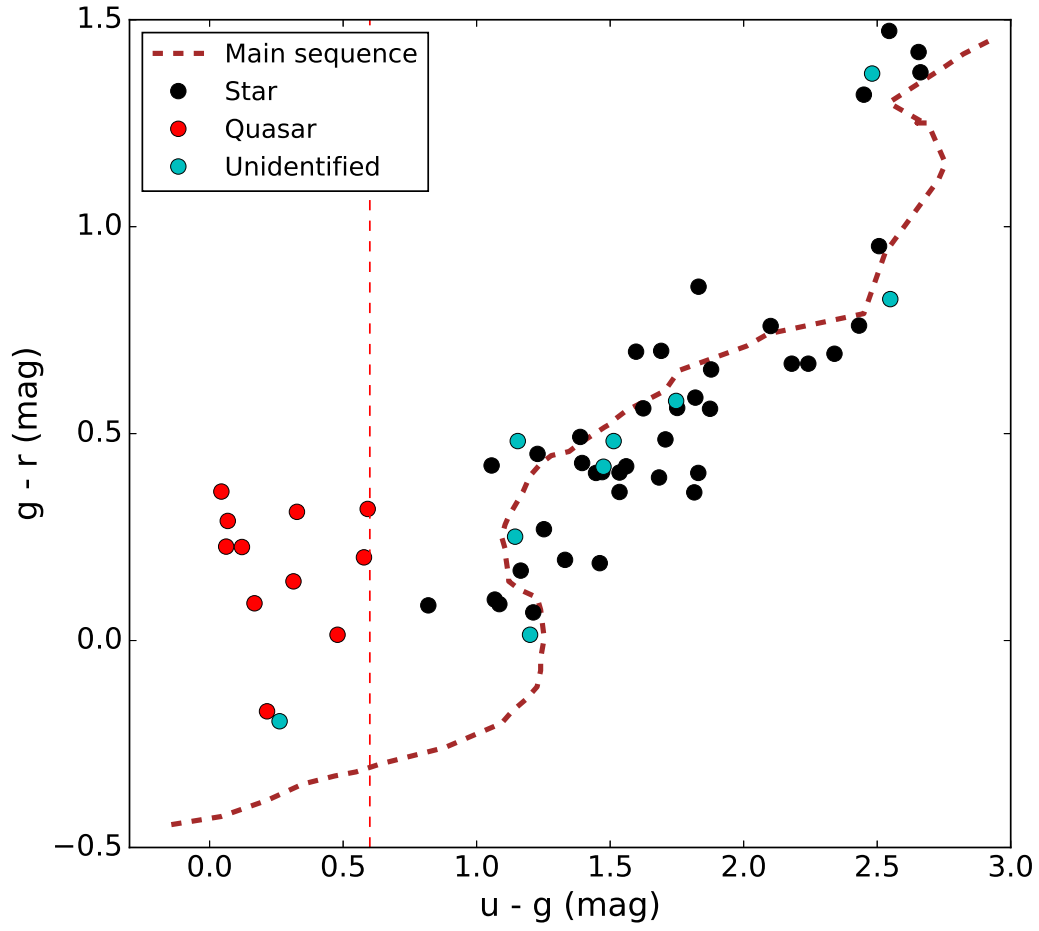


Fig. 5.—: The  $g - r$  vs.  $u - g$  color-color diagram of u-band variable sources. The red, black and blue dots represent quasars, stars and unidentified sources, respectively (same below). The brown dashed line represents the position of main-sequence. The red dashed line represents the line of quasar criteria of  $u - g = 0.6$ .

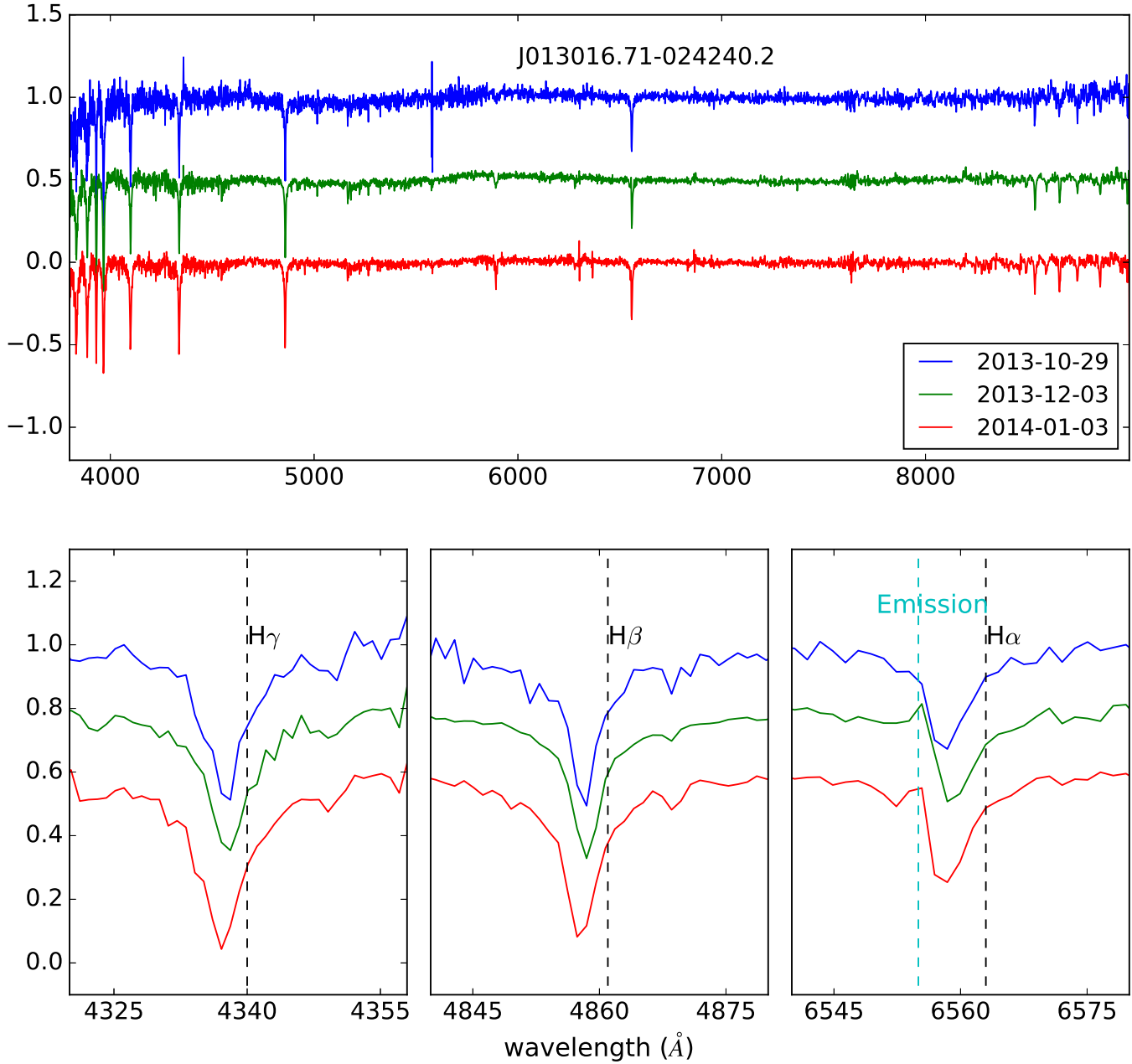


Fig. 6.—: The top panel shows three normalized spectra at different nights. The bottom panels shows Balmer absorption lines and the vertical black dashed show the restframe wavelength of spectral lines. The vertical shallow blue dashed in the right picture shows the position of fill-in H $\alpha$  emission.

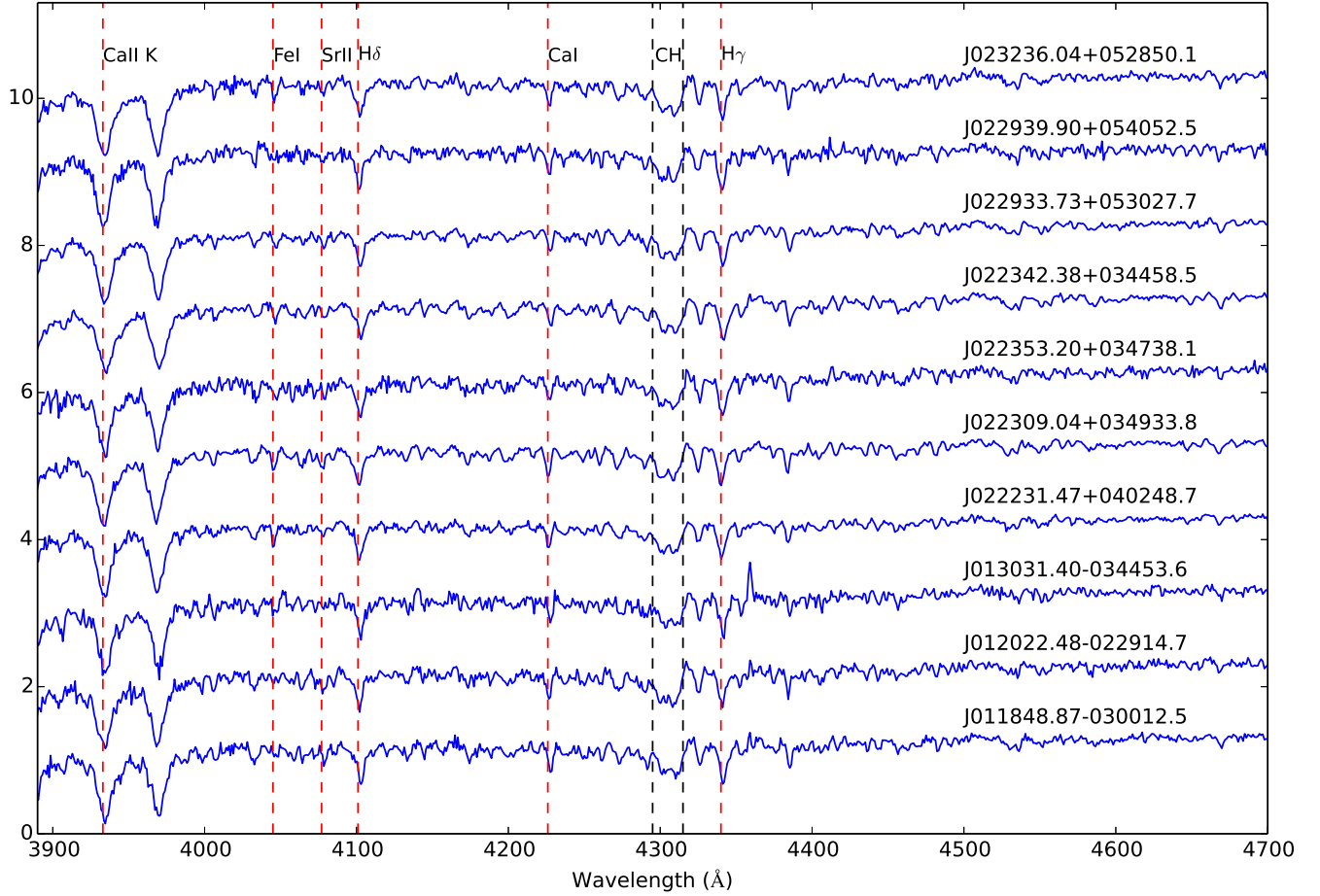


Fig. 7.—: The spectra of 10 objects whose spectrum have similar features. The molecule CH (from  $\lambda 4295$  to  $\lambda 4315$ ) is wide, and shown between two black dashed lines. The red lines represent other the positions of other lines.

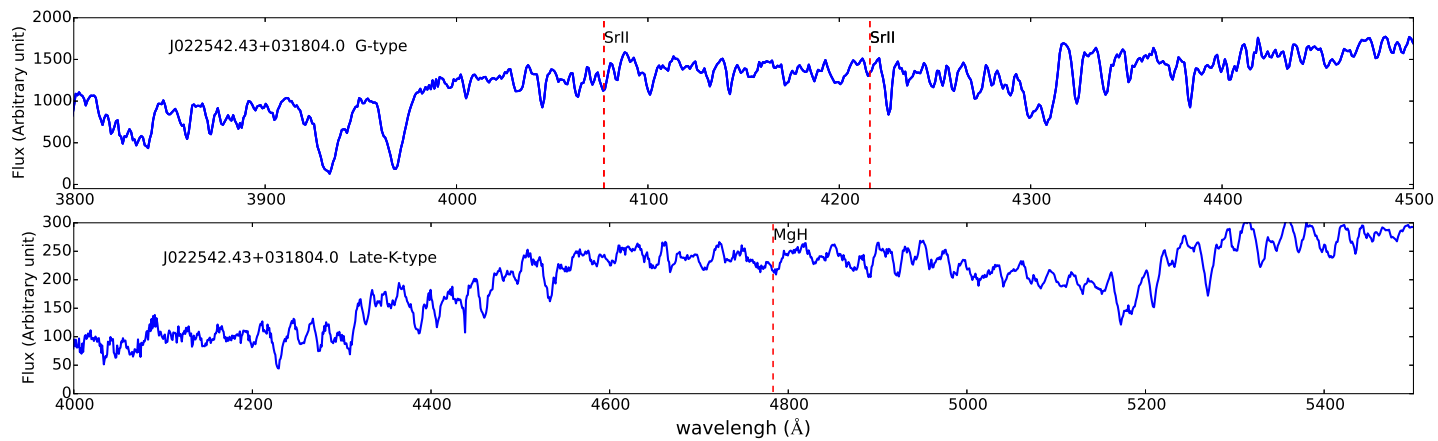


Fig. 8.—: The example spectra of G-type and late-K-type stars. The upper is a G-type star with SrII features and the lower is a late K-type star with MgH feature.

Table 1. Characteristic Color of Different Types of Stars

Target Type	Color Seleccion <sup>a</sup>
RR Lyrae candidate <sup>b</sup>	$0.98 < (u - g) < 1.30$ and $-0.05 < RR1 < 0.35$ and $0.06 < RR2 < 0.55$ and $-0.15 < (r - i) < 0.22$ and $-0.21 < (i - z) < 0.25$
sdO/sdB/white dwarf <sup>c</sup>	$-0.1 < (g - r) < -0.2$ and $-0.1 < (u - g) < 0.7$ and $u - g + 2 * (g - r) < -0.1$
AGB <sup>c</sup>	$2.5 < (u - g) < 3.5$ and $0.9 < (g - r) < 1.3$ and $s < -0.06$
k gaint <sup>c</sup>	$0.7 < (u - g) < 4.0$ and $0.35 < (g - r) < 0.7$ and $0.15 < (r - i) < 0.6$ and $l > 0.07$
Low metallicity <sup>c</sup>	$-0.5 < (g - r) < 0.75$ and $0.6 < (u - g) < 3.0$ and $l > 0.135$

<sup>a</sup>The color adopted in selection are defined below :

$$RR1 = 0.45 * (u - g) - (g - r) - 0.12$$

$$RR2 = (u - g) + 0.67 * (g - r) - 1.07$$

$$s = -0.249 * u + 0.795 * g - 0.555 * r + 0.124$$

$$l = -0.436 * u + 1.129 * g - 0.119 * r - 0.574 * i + 0.1984$$

<sup>b</sup>Using color from Sesar et al. 2007.

<sup>c</sup>Using color from Yanny et al. 2009.

Table 2. The General Properties of the u-band Variable objects

Name	RA (°)	Dec (°)	u <sub>SCUSS</sub>	date (UTC)	u <sub>SDSS</sub>	date (UT)	g <sub>SDSS</sub>	r <sub>SDSS</sub>	Redshift	Type <sup>a</sup>	T <sub>eff</sub>	log <sub>g</sub>
J023418.41+042322.7	38.576725	4.3896499	18.552 ±0.009	2012-12-09	18.346 ±0.029	2008-10-03	17.867 ±0.025	17.853 ±0.025	0.671 ±0.001	quasar	—	—
J023044.21+025220.0	37.6842194	2.8722501	18.042 ±0.004	2013-12-01	18.287 ±0.029	2008-09-06	17.695 ±0.029	17.377 ±0.021	0.937 ±0.001	quasar	—	—
J022544.29+012541.7	36.4345703	1.428275	18.108 ±0.007	2013-01-09	18.444 ±0.020	2008-10-03	18.323 ±0.025	18.097 ±0.039	0.996 ±0.004	quasar	—	—
J022253.26+033421.1	35.7219238	3.5725334	17.925 ±0.003	2013-12-26	17.673 ±0.019	2009-09-16	17.505 ±0.025	17.415 ±0.016	1.601 ±0.003	quasar	—	—
J013515.24-021349.4	23.8135242	-2.2304027	17.584 ±0.004	2013-10-25	17.816 ±0.024	2008-10-31	17.754 ±0.024	17.527 ±0.016	1.818 ±0.002	quasar*	—	—
J013405.10-031012.3	23.521265	-3.1700835	17.866 ±0.005	2013-11-07	18.210 ±0.026	2008-10-31	18.142 ±0.033	17.853 ±0.016	1.235 ±0.003	quasar	—	—
J013139.56-025456.2	22.914854	-2.9156139	18.177 ±0.006	2013-10-25	18.413 ±0.105	2008-10-30	18.086 ±0.019	17.775 ±0.024	1.008 ±0.003	quasar	—	—
J012907.40-033844.3	22.2808456	-3.6456554	17.911 ±0.004	2013-11-03	18.267 ±0.023	2008-10-31	18.223 ±0.028	17.863 ±0.019	1.385 ±0.002	quasar	—	—
J012602.99-000822.5	21.5124702	-0.1396056	17.921 ±0.004	2013-11-03	18.427 ±0.020	2001-11-18	18.113 ±0.025	17.97 ±0.010	0.402 ±0.001	quasar*	—	—
J012302.02-024400.3	20.7584324	-2.7334332	17.627 ±0.004	2013-12-05	17.840 ±0.017	2009-01-16	17.625 ±0.024	17.796 ±0.020	0.439 ±0.001	quasar*	—	—
J012240.12-003239.7	20.6671867	-0.5443611	18.426 ±0.005	2013-12-05	18.710 ±0.033	2004-09-24	18.132 ±0.021	17.931 ±0.018	0.886 ±0.003	quasar*	—	—
J023830.53+034458.0	39.6272469	3.7494667	18.494 ±0.006	2013-10-02	17.915 ±0.018	2008-10-08	16.750 ±0.020	16.581 ±0.018	—	A7IV/F0/RR Lyr	5812.05 ±449.91	3.657 ±1.26
J023410.98+054031.5	38.5457878	5.6754303	18.478 ±0.005	2013-12-26	18.754 ±0.034	2005-10-12	16.653 ±0.026	15.893 ±0.020	—	G5/G8/-	4991.17 ±207.94	4.538 ±0.403
J023236.04+052850.1	38.1500549	5.4804583	15.855 ±0.002	2014-01-05	16.332 ±0.030	2009-09-16	15.092 ±0.024	14.37 ±0.034	—	G0/G0/-	5882.35 ±255.62	4.368 ±0.563
J023232.80+043605.7	38.1366959	4.6015997	16.640 ±0.002	2014-01-05	16.887 ±0.021	2008-10-03	15.263 ±0.028	14.702 ±0.029	—	G3/G3/-	5441.25 ±263.21	3.883 ±0.741
J023151.39+015057.1	37.9641304	1.8492193	16.147 ±0.002	2013-12-01	16.404 ±0.03	2008-10-03	15.117 ±0.022	14.737 ±0.06	—	F9/F9/-	5746.46 ±260.2	4.491 ±0.536
J023043.78+041514.3	37.6824493	4.2539721	18.741 ±0.007	2013-12-01	18.505 ±0.022	2008-10-08	15.960 ±0.028	14.487 ±0.014	—	M/-/dwarf	—	—
J022956.29+053530.6	37.4845581	5.5918474	18.856 ±0.005	2012-10-13	19.136 ±0.045	2004-12-14	17.805 ±0.027	17.61 ±0.025	—	A/-/-	—	—
J022949.10+053557.8	37.4546127	5.5993972	18.158 ±0.004	2013-01-06	18.508 ±0.041	2004-12-14	16.973 ±0.027	16.614 ±0.025	—	F7/F7/-	5924.64 ±312.95	4.202 ±0.565
J022944.30+054056.6	37.4346161	5.6823969	18.466 ±0.008	2013-01-06	18.844 ±0.043	2004-12-14	16.412 ±0.027	15.651 ±0.025	—	G8/K0/-	5128.96 ±140.81	4.531 ±0.366
J022939.90+054052.5	37.4162865	5.681272	16.216 ±0.003	2013-12-01	16.571 ±0.039	2004-12-14	15.011 ±0.027	14.59 ±0.025	—	F6/F2/-	5971.51 ±256.22	4.197 ±0.559
J022933.73+053027.7	37.3905525	5.5077028	16.977 ±0.003	2013-12-01	17.335 ±0.040	2004-12-14	15.800 ±0.027	15.394 ±0.025	—	G1/F7/-	5901.83 ±252.71	4.194 ±0.56
J022925.40+053105.0	37.3558655	5.5180745	17.192 ±0.003	2012-11-13	17.490 ±0.040	2004-12-14	16.029 ±0.027	15.842 ±0.025	—	F5/F0/-	6975.91 ±309.96	4.262 ±0.38
J022922.73+054104.5	37.3447151	5.6845999	17.045 ±0.003	2013-10-30	17.254 ±0.039	2004-12-14	15.859 ±0.025	15.430 ±0.024	—	F9/G0/-	5657.46 ±396.87	3.757 ±0.797
J022921.90+053316.3	37.3412819	5.5545392	16.837 ±0.002	2013-12-01	17.088 ±0.039	2004-12-14	15.381 ±0.025	14.895 ±0.024	—	G4/G7/-	5628.7 ±275.8	4.131 ±0.57
J022914.57+053407.4	37.3107262	5.5687275	16.241 ±0.002	2014-01-05	16.449 ±0.039	2004-12-14	14.631 ±0.025	14.115 ±0.024	—	G3/G5/-	5585.42 ±189.57	4.153 ±0.546
J022757.57+052457.9	36.9898796	5.4160862	18.312 ±0.006	2013-12-01	18.099 ±0.027	2009-09-16	15.437 ±0.023	14.064 ±0.021	—	M/-/M dwarf	—	—
J022751.64+034503.2	36.9651985	3.7509055	17.138 ±0.002	2013-12-26	17.571 ±0.026	2009-09-16	15.409 ±0.023	14.389 ±0.023	—	K0/K1/-	5070.75 ±79.48	4.599 ±0.32
J022727.49+031054.8	36.8645668	3.1819	18.018 ±0.004	2013-10-02	17.498 ±0.019	2008-09-06	15.159 ±0.015	14.053 ±0.001	—	M /-/M dwarf+	—	—

Table 2—Continued

Name	RA (°)	Dec (°)	u <sub>SCUSS</sub>	date (UTC)	u <sub>SDSS</sub>	date (UT)	g <sub>SDSS</sub>	r <sub>SDSS</sub>	Redshift	Type <sup>a</sup>	T <sub>eff</sub>	log <sub>g</sub>
J022611.71+031011.5	36.5487976	3.1698694	17.542 ±0.003	2013-12-01	18.042 ±0.047	2009-09-16	15.862 ±0.024	15.193 ±0.022	—	G7/G8/–	5068.55 ±214.5	3.801 ±0.574
J022602.18+025814.4	36.5090904	2.9706779	18.393 ±0.004	2013-10-02	18.641 ±0.031	2008-10-03	16.134 ±0.016	15.181 ±0.02	—	G7/K5/AGB*	4596.76 ±90.82	4.715 ±0.252
J022558.05+031132.6	36.4918976	3.1923974	16.408 ±0.002	2013-01-09	16.839 ±0.046	2009-09-16	14.850 ±0.024	14.194 ±0.001	—	G8/G5/–	5108.47 ±98.81	3.466 ±0.625
J022553.64+031049.9	36.4735222	3.1805501	17.650 ±0.003	2013-10-02	17.912 ±0.047	2009-09-16	16.093 ±0.024	15.506 ±0.022	—	G8/G7/–	5358.32 ±176.85	4.528 ±0.486
J022552.56+031425.1	36.4690056	3.2403224	17.927 ±0.003	2013-12-26	18.287 ±0.048	2009-09-16	16.552 ±0.024	16.013 ±0.022	—	G2/G3/–	5274.4 ±228.15	4.406 ±0.51
J022542.43+031804.0	36.4268227	3.3011334	17.784 ±0.003	2013-01-09	18.084 ±0.032	2009-09-16	16.614 ±0.014	16.207 ±0.015	—	G3/F9/–	5942.6 ±252.22	4.631 ±0.441
J022541.21+031523.9	36.4217224	3.2566583	17.364 ±0.003	2013-10-02	17.946 ±0.047	2009-09-16	15.606 ±0.024	14.913 ±0.022	—	G9/G8/–	5343.25 ±134.38	4.688 ±0.406
J022445.76+032812.1	36.1906891	3.4700305	17.766 ±0.003	2013-12-26	18.090 ±0.071	2009-09-16	16.558 ±0.022	16.115 ±0.009	—	G0/G2/–	5904.52 ±413.6	4.55 ±0.931
J022439.18+033258.0	36.1632729	3.5494637	18.820 ±0.006	2013-12-26	19.216 ±0.073	2009-09-16	16.854 ±0.022	16.127 ±0.009	—	G7/G7/–	5110.81 ±231.75	4.559 ±0.418
J022428.67+033223.5	36.1194649	3.5398805	18.030 ±0.005	2013-10-02	18.546 ±0.071	2009-09-16	16.672 ±0.022	16.112 ±0.009	—	G8/G7/–	5417.57 ±228.35	4.769 ±0.478
J022353.20+034738.1	35.9716988	3.7939305	17.734 ±0.003	2013-12-26	17.975 ±0.015	2009-09-16	16.528 ±0.012	16.123 ±0.014	—	G2/F7/–	5895.04 ±263.23	4.203 ±0.64
J022350.74+034437.6	35.9614182	3.7438056	18.266 ±0.004	2013-12-26	18.738 ±0.072	2009-09-16	16.496 ±0.016	15.827 ±0.025	—	K1/G9/–	5119.65 ±161.25	4.522 ±0.431
J022342.38+034458.5	35.9265823	3.7495973	16.177 ±0.002	2013-01-05	16.601 ±0.071	2009-09-16	14.898 ±0.015	16.887 ±0.032	—	G2/G0/–	6090.33 ±151.68	4.37 ±0.489
J022341.57+034442.3	35.923233	3.7450917	16.723 ±0.002	2012-11-14	17.155 ±0.071	2009-09-16	15.271 ±0.016	14.070 ±0.001	—	F6/F9/–	5593.81 ±171.41	4.479 ±0.509
J022326.86+034637.2	35.8619308	3.7770195	17.666 ±0.003	2013-01-06	17.990 ±0.071	2009-09-16	15.841 ±0.016	15.224 ±0.002	—	K2/K0/–	5279.59 ±126.79	4.425 ±0.434
J022325.59+035036.2	35.8566437	3.8433971	17.991 ±0.003	2013-12-01	18.331 ±0.072	2009-09-16	16.580 ±0.016	16.018 ±0.025	—	G8/G5/–	5610.74 ±180.87	4.649 ±0.486
J022324.12+034917.9	35.8505325	3.8216584	16.231 ±0.002	2012-11-14	16.638 ±0.07	2009-09-16	14.667 ±0.015	14.059 ±0.001	—	F8/F9/–	5416.3 ±121.23	4.46 ±0.478
J022323.90+035338.5	35.8495827	3.8940361	18.086 ±0.004	2013-10-30	18.398 ±0.017	2009-09-16	16.520 ±0.012	15.865 ±0.014	—	G8/G7/–	5221.7 ±243.34	3.666 ±0.7
J022316.03+035124.1	35.8168106	3.8567026	16.450 ±0.002	2013-12-26	16.900 ±0.071	2009-09-16	14.782 ±0.015	14.116 ±0.001	—	G8/G7/–	5207.6 ±112.99	4.616 ±0.42
J022309.04+034933.8	35.7876816	3.8260748	16.278 ±0.002	2013-12-01	16.561 ±0.070	2009-09-16	15.040 ±0.016	17.014 ±0.056	—	G4/G2/–	5977.43 ±149.89	4.355 ±0.507
J022302.97+020939.4	35.762394	2.1609502	16.569 ±0.003	2013-12-01	16.800 ±0.036	2008-10-03	15.459 ±0.036	15.023 ±0.050	—	G6/G3/–	5573.42 ±214.96	4.524 ±0.534
J022231.47+040248.7	35.6311302	4.0468779	16.146 ±0.002	2013-01-08	16.636 ±0.035	2009-09-16	14.953 ±0.017	14.559 ±0.013	—	G3/G0/–	5867.2 ±193.08	4.166 ±0.609
J013412.46-013427.5	23.5519257	-1.5743166	18.276 ±0.005	2013-12-03	18.051 ±0.025	2008-10-30	15.601 ±0.014	14.282 ±0.028	—	M/–/M dwarf	—	—
J013352.87-004502.6	23.470295	-0.7507361	18.856 ±0.009	2013-12-05	18.300 ±0.023	2003-11-20	17.215 ±0.019	17.127 ±0.013	—	A8III/F0/RRLyrr	6215.14 ±419.92	4.597 ±0.417
J013318.45-012720.1	23.3268909	-1.4555889	18.124 ±0.005	2013-11-03	17.697 ±0.018	2008-10-31	16.485 ±0.016	16.417 ±0.013	—	F/F0/RRLyrr	6174.39 ±305.13	4.164 ±0.511
J013130.13-013214.6	22.8755569	-1.5374084	18.502 ±0.007	2014-01-03	18.213 ±0.026	2008-10-31	15.820 ±0.024	14.779 ±0.019	—	K7/K5/V*	4313.16 ±85.22	4.358 ±0.279
J013031.40-034453.6	22.6308327	-3.748225	18.742 ±0.005	2013-11-03	18.308 ±0.029	2008-12-30	17.252 ±0.03	16.829 ±0.016	—	F9/F8/–	6015.54 ±235.89	4.351 ±0.473
J013016.71-024240.2	22.5696545	-2.7111723	16.269 ±0.002	2013-10-29	15.915 ±0.020	2008-10-31	14.756 ±0.021	14.611 ±0.001	—	F0/F0/ RR Lyrr	5995.88 ±269.78	4.021 ±0.568
J012915.36-025553.2	22.3140125	-2.9314556	17.319 ±0.003	2013-12-03	17.526 ±0.012	2008-10-30	15.695 ±0.024	14.840 ±0.018	—	K3/K3/–	4864.59 ±79.36	3.944 ±0.368



Table 2—Continued

Name	RA (°)	Dec (°)	u <sub>SCUSS</sub>	date (UTC)	u <sub>SDSS</sub>	date (UT)	g <sub>SDSS</sub>	r <sub>SDSS</sub>	Redshift	Type <sup>a</sup>	T <sub>eff</sub>	log <sub>g</sub>
J012752.98-032635.0	21.9707565	-3.443064	18.116 ±0.005	2013-10-25	18.331 ±0.023	2008-10-31	17.079 ±0.025	16.810 ±0.034	---	F5/F0/RRLyr	5836.9 ±314.49	3.631 ±0.831
J012545.85-004742.0	21.4410629	-0.7950194	17.662 ±0.003	2013-10-29	18.643 ±0.067	2003-11-20	15.499 ±0.027	14.551 ±0.019	---	K0/K5/-	4523.2 ±67.22	4.629 ±0.233
J012352.90-012241.5	20.9704208	-1.3782084	18.581 ±0.007	2013-12-27	18.372 ±0.024	2008-10-31	15.717 ±0.014	14.295 ±0.012	---	M/-/M dwarf	---	---
J012344.90-001242.9	20.9371166	-0.2119194	17.313 ±0.003	2013-10-29	17.053 ±0.024	2003-11-20	15.362 ±0.022	14.662 ±0.023	---	G8/K0/gaint*	5020.74 ±106.14	4.609 ±0.344
J012340.10-001324.2	20.9170999	-0.2234056	18.232 ±0.006	2013-11-03	17.981 ±0.026	2003-11-20	17.162 ±0.022	17.077 ±0.023	---	A/-/HB*	---	---
J012324.70-010704.1	20.8529301	-1.1178167	16.590 ±0.002	2014-01-09	16.812 ±0.029	2003-11-20	15.424 ±0.021	14.932 ±0.013	---	G9/G8/-	5424.32 ±168.26	4.617 ±0.468
J012316.78-003512.6	20.8199348	-0.5868361	18.322 ±0.005	2013-12-05	19.097 ±0.077	2001-09-18	17.267 ±0.021	16.862 ±0.015	---	G/-/-	---	---
J012222.67-002012.8	20.5944881	-0.3368917	18.541 ±0.005	2013-11-03	17.891 ±0.031	2003-10-19	16.877 ±0.024	16.346 ±0.022	---	G3/F0/-	5587.11 ±208.86	4.127 ±0.603
J012025.81-012920.4	20.1075497	-1.4890195	18.215 ±0.006	2013-11-07	19.050 ±0.074	2008-10-31	17.235 ±0.024	16.877 ±0.012	---	F5/F0/-	6175.75 ±270.61	4.204 ±0.462
J012022.48-022914.7	20.0936794	-2.4874222	18.225 ±0.006	2013-11-07	18.007 ±0.023	2008-10-30	16.779 ±0.017	16.328 ±0.015	---	G3/G0/-	5809.82 ±235.0	4.047 ±0.643
J011848.87-030012.5	19.7036362	-3.0034778	17.480 ±0.004	2013-11-07	17.755 ±0.021	2001-11-11	16.257 ±0.021	15.829 ±0.01	---	G1/F9/-	5840.47 ±200.63	4.268 ±0.549
J011741.77-012422.9	19.4240532	-1.4063694	18.111 ±0.005	2013-10-25	18.463 ±0.027	2008-10-31	16.866 ±0.018	16.168 ±0.018	---	G2/G7/-	5163.18 ±132.06	4.5 ±0.45
J011709.54-021318.2	19.2897625	-2.2217417	18.66 ±0.01	2013-11-07	18.880 ±0.027	2008-10-31	17.812 ±0.014	17.713 ±0.016	---	A1IV/-/RRLyr*	---	---
J023831.91+030933.6	39.632981	3.1593502	18.168 ±0.006	2013-01-06	17.913 ±0.022	2008-09-06	17.651 ±0.017	17.846 ±0.018	---	unidentified	---	---
J023815.35+030800.7	39.563972	3.1335295	18.913 ±0.009	2013-10-30	18.689 ±0.02	2008-09-06	16.208 ±0.014	14.838 ±0.014	---	unidentified	---	---
J022944.83+053721.0	37.436792	5.6225182	18.320 ±0.005	2012-10-13	18.682 ±0.042	2004-12-14	17.207 ±0.027	16.787 ±0.025	---	unidentified	---	---
J022803.74+014932.9	37.015621	1.8258154	17.667 ±0.003	2013-10-30	17.300 ±0.019	2008-10-03	16.100 ±0.018	16.086 ±0.015	---	unidentified/RRLyr*	---	---
J022748.45+042834.5	36.951904	4.4762608	18.744 ±0.005	2013-12-26	18.516 ±0.037	2008-10-03	17.801 ±0.017	17.472 ±0.024	---	unidentified	---	---
J022447.56+032608.7	36.198182	3.4357571	16.218 ±0.002	2014-01-05	16.503 ±0.070	2009-09-16	15.024 ±0.022	15.298 ±0.002	---	unidentified	---	---
J022420.03+033027.8	36.083472	3.5077244	18.010 ±0.005	2014-01-05	18.251 ±0.071	2009-09-16	15.702 ±0.022	14.877 ±0.009	---	unidentified	---	---
J022219.15+040233.3	35.57979	4.0425862	17.269 ±0.003	2013-12-01	17.578 ±0.036	2009-09-16	16.065 ±0.017	15.583 ±0.014	---	unidentified	---	---
J022213.77+040535.8	35.557383	4.0933007	18.645 ±0.006	2013-12-26	18.975 ±0.040	2009-09-16	17.228 ±0.017	16.649 ±0.014	---	unidentified	---	---
J013156.26-023100.7	22.984421	-2.5168671	17.487 ±0.003	2013-11-07	17.758 ±0.020	2008-10-30	16.604 ±0.016	16.122 ±0.03	---	unidentified	---	---
J011742.01-020819.8	19.425079	-2.1388566	16.926 ±0.003	2013-11-07	17.335 ±0.026	2001-11-11	16.191 ±0.022	15.94 ±0.018	---	unidentified/RRLyr	---	---

<sup>a</sup>For quasars, the ones which have been found in NED or SDSS are marked with asterisk. For stars, there are three types are marked in table including: (1) spectral types cross-matched with MILES; (2) spectral types cross-matched with LAMOST DR1; (3) stellar types identified by SIMBAD, color selection (asterisk) or spectral inspection (plus). Due to the low SNR, 11 variable sources can not be identified by MILES or LAMOST DR1.